# Discovery of necklace-like links made of dislocations

Pawel Pieranski, Maria Helena Godinho

# Discovery of necklace-like links made of dislocations

**Pawel Pieranski**[a,2] **and Maria Helena Godinho**[b]

This manuscript was compiled on December 8, 2024

**Complex knotted and at the same time linked entanglements of linear topological defects such as vortices in superfluids, disclinations in nematics or dislocations in cholesterics can be generated during symmetry-breaking phase transitions or by mechanical perturbations. In superfluids and in nematics, such dense entanglements are known to untie, by rewiring of their crossings, into independent unknots that finally shrink and collapse. We point out that in cholesterics confined in gaps with variable thickness, the decay of initially dense entanglements of dislocations can be incomplete. Instead of leading to the defect-less state it produces a new category of necklace-like links which consists of many minimal loops tethered on kinks of much larger cargo loops. We show in particular how a necklace with T minimal loops is generated by rewiring of a two components tangle [2T] with numerator closure. This process conserves the linking number T.**

Dislocations | Knots | Links | Topological metadefetcs | Cholesterics | ...

For topological reasons, the linear topological defects (1, 2) such as vortices in superfluids (3, 4), disclinations in nematics (5–7) or dislocations in cholesterics (2, 7, 8) must form closed loops when they do not end on surfaces.

From the mathematical point of view, these loops, considered as one-dimensional lines embedded in a three-dimensional space, can be equivalent to unknots, knots, or links (9, 10).

The symmetry-breaking normal fluid → superfluid, isotropic liquid → nematic and isotropic liquid → cholesteric phase transitions are known to generate knotted and at the same time linked entanglements of, respectively, vortices, disclinations and dislocations.

Decay of such topologically complex entanglements attracted much attention both from the theoretical and experimental points of view and, among others, the following two questions were raised (4, 11): (1°) What is the terminal state of the decay ? (2°) What is the topological pathway leading to it ?

## Decay of the entangled vortices in superfluids and of disclinations in nematics into the defect-less ground state

Previous studies of disclinations in nematics (12, 13) (see also the SI Appendix section "Topological decay of entanglements of disclinations in nematics") and of vortices in superfluids (4, 11, 14) (see the SI Appendix section "Topological decay of entanglements of superfluid vortices") have shown that, inside a simply connected bulk, arbitrarily knotted and linked entanglements are rewired into systems of independent loops that finally collapse. The paradigmatic conclusion of these studies is thus that the topological decay of the entangled linear topological defects leads to the defect-less ground state.

## Decay of the entangled dislocations in cholesterics into the necklace state

In this paper we will point out that the decay of the dense entanglements of dislocations in cholesterics of pitch $p$ confined inside a cylinder/cylinder gap is incomplete because it leads

### Significance Statement

Knots and links made of one-dimensional lines embedded in a three-dimensional space are archetypes of topological intricacies. Physical knots and links can be, remarkably, tied from linear singularities such as vortices in superfluids or linear defects in liquid crystals. This article reports on the discovery of a *new category of links dubbed necklaces* occurring in cholesteric liquid crystals. They are made of small dislocation loops tethered on much larger loops. Necklaces are remnants of the decay of the dense entanglements of dislocations produced during the symmetry breaking isotropic → cholesteric phase transition. Necklaces are ubiquitous but they remained hidden from view for decades because the tethered loops are usually too small for observation in an optical microscope.

Author affiliations: [a]Laboratoire de Physique des Solides, Université Paris-Saclay, Orsay, France; [b]i3N/CENIMAT, Department of Materials Science, NOVA School of Science and Technology, NOVA University Lisbon, Campus de Caparica, Caparica 2829 - 516, Portugal

[1]P.P. contributed equally to this work with M.H.G.

[2]To whom correspondence should be addressed. E-mail: pawel.pieranski@universite-paris-saclay.fr

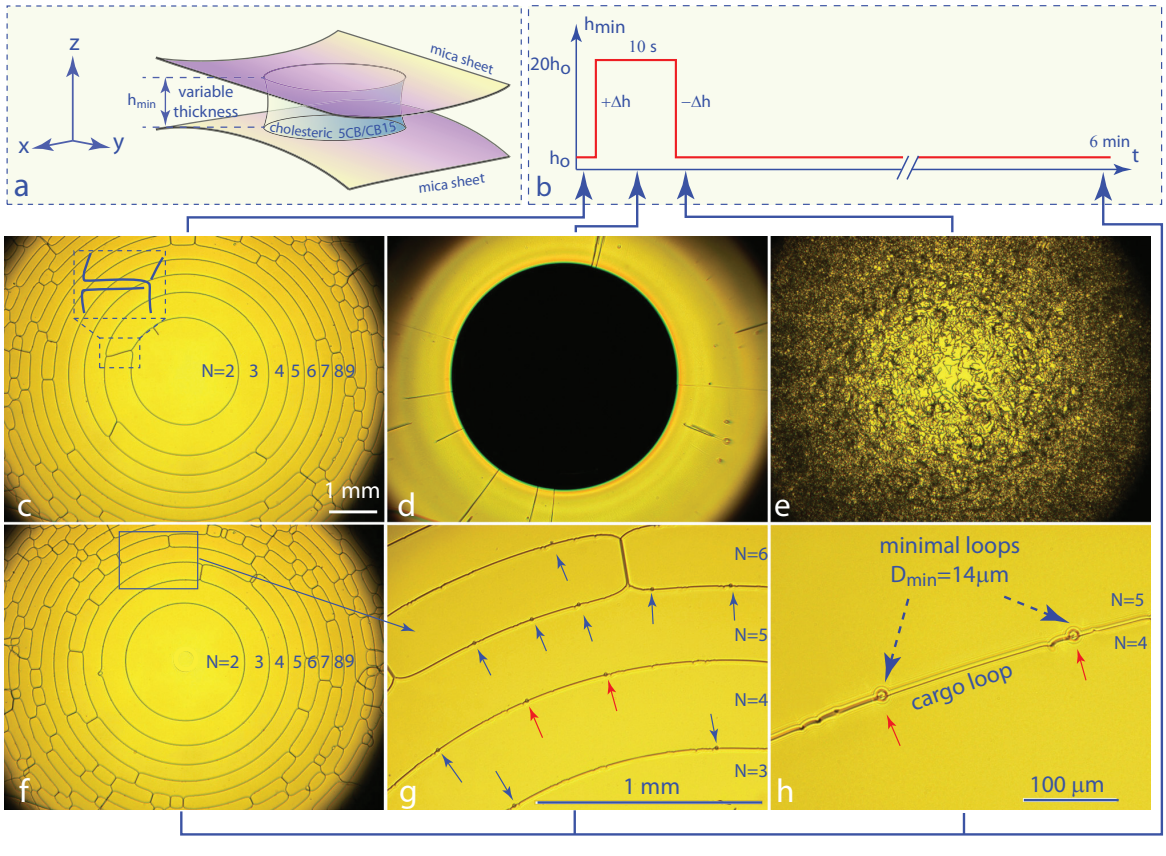


**Fig. 1.** Generation of the necklace state by a dilation-compression strain pulse. a) Geometry of the experiment: cylindrical mica sheets separated by the distance $h_{min}$. b) The dilation-compression strain pulse. c-h) Pictures taken in a microscope. c) The initial ground state made of concentric circular dislocations. N is the number of full cholesteric pitches contained between the mica sheets. d) Reduction of the diameter of the cholesteric droplet after a sudden increase by $\Delta h$ of the minimal gap thickness $h_{min}$ between the mica sheets. e) Droplet after a sudden compression restoring the initial thickness. It contains a dense tangle of dislocations generated by the strain pulse. f) After 6 minutes of relaxations the droplet seems to be again in the ground state made of concentric circular dislocations. g) At higher magnification, 11 minimal loops tethered on circular dislocations become apparent in the rectangular area defined in (f). h) Close-up view of the two minimal loops pointed with red arrows in the picture (g). The total number of the minimal loops in the picture (f) is of the order of 200. (Sample composition: 0.86% of 15CB in 5CB.)

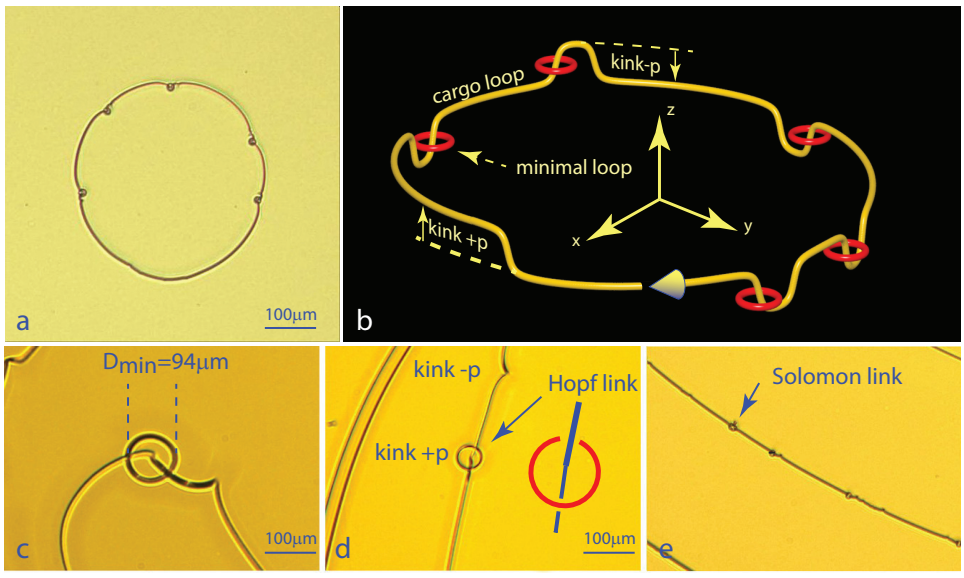


**Fig. 2.** Geometry of the necklace state. a) View in a microscope of a necklace made of one circular cargo loop charged with five minimal loops. b) Perspective view of the necklace. The minimal loops are tethered on $+p$ kinks which in a first approximation can be seen as vertical screw dislocations of length $p$. c-e) The diameter of the minimal loops is of the order of the cholesteric pitch p : $D_{min} \approx p$. It varies with the concentration $c_{15CB}$ of the chiral compound CB15 in the nematic 5CB: (c) $c_{15CB} = 0.4\%$, (d) $c_{15CB} = 0.86\%$ (e) $c_{15CB} = 3.4\%$. e) Occurrence (very scarce) of the Solomon configuration of the necklace state. The minimal loop indicated by the arrow is tethered on the cargo loop in a different manner detailed in the Figure 4a.

not the defect-less ground state but to a more complex state, represented in Figures 1 and 2, in which large dislocation loops called *cargo loops*) carry numerous small loops, of the same radius $r_{ml} \approx p/2$, called *minimal loops*. For obvious reasons we dubbed it *the necklace state*.

For experts in liquid crystals, at a first sight, the patterns of dislocations in Figures 1c and f are nothing else but the widely known Grandjean-Cano patterns (8, 15, 16) made of dislocations parallel to lines of equal thickness $h(x, y) = const$. Inside the gap between the cylindrical mica sheets of the same radius of curvature $R_m$ (see Figure 1a), they are circular because $h(x, y) \approx h_{min} + (x^2 + y^2)/(2R_m) = h_{min} + r^2/(2R_m)$.

In samples with the cholesteric pitch $p < 1\mu m$, the minimal loops are so small that they cannot be resolved in an optical microscope. For this reason, probably, the necklace state remained hidden from identification for decades.

## Genesis of the necklace state

The knotted and at the same linked dense entanglements of dislocations can be generated either through the isotropic-cholesteric phase transition as mentionned above or by a dilation-compression pulse-like perturbation (see Figures 1a and b) applied to the cholesteric layer confined between cylindrical surfaces. The case of the thermal genesis is more complicated to analyze because two types of dislocations with Burgers vectors b=p and b=p/2 (defined in the SI Appendix Section "Two types of dislocations") are generated simultaneously. We will consider it in the SI Appendix Section "Topological decay of entanglements of dislocations produced by the Isotropic-Cholesteric phase transition". As in the second case of the mechanical excitation only the b=p dislocations are generated, we consider it here.

**Generation of dense entanglements of dislocations by a dilation-compression strain pulse.** The strain pulse, applied to the ground state of the cholesteric layer confined between the crossed cylindrical mica sheets (see Figures 1a and b), starts by an increase $+\Delta h$ of the gap thickness . This results in a reduction of the diameter of the droplet (see Figure 1d) which must conserve its volume. In a first approximation, the elongation of the droplet in the z direction is accompanied by a converging radial (Poiseuille) flow in the (x,y) plane that convects the dislocation loops. Simultaneaously, the cholesteric helices are stretched in the z direction. For example, in the center of the droplet where $N = 2$, the pitch p increases from $h_{min}/2$ to $(h_{min} + \Delta h)/2$. Typically, when $\Delta h \approx 20 h_{min}$, the pitch p is elongated by the factor of the order of 20 which is more than enough to trigger both the undulation instability and the nucleation of dislocation antiloops (17, 18). In practice, the texture of the droplet is perturbed so much that it looses its initial transparency (see Figure 1c).

The subsequent compression $-\Delta h$ restores the diameter of the droplet but not its initial transparency because the compressive strain generates a dense entanglement made *exclusively* of the $b = p$ dislocations (defined in the SI Appendix Section "Two types of dislocations" ). In this entangled state, initially, the total length of dislocations per unit area is larger than that of the ground state by a factor of the order of 100.

**Elastic relaxation, topological decay of the entanglements of the $b = p$ dislocations into the necklace state.** After 6 minutes of relaxation driven by the orientational elasticity of the cholesteric, the topological decay of the entanglement apparently restores the ground state (see Figure 1f) of the cholesteric droplet. However, a higher magnification (see Figure 1g) unveils numerous small circular loops of the same size, $D_{min} = 14\mu m$ (see Figure 1h), tethered on the circular concentric dislocations of the initial ground state.

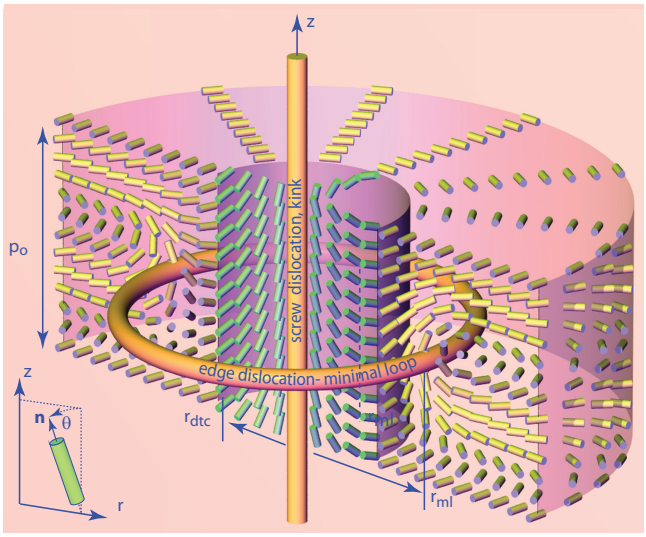


**Fig. 3.** Director field in the vicinity of a minimal loop tethered on a kink of a cargo loop (see the Appendix Section "Diameter of the minimal loops").

## Features of the necklace state

**Geometry of the necklace state, cargo loops.** The most important feature of the necklace state well visible in Figures 2b and 3 (see also Figure S5 of the SI) is that *the circular minimal loops are tethered on quasi vertical segments of the cargo loop called kinks* + $p$ (16, 19).

The cargo loops of the necklace state keep their large circular size thanks to the elastic interaction with the cylindrical mica sheets imposing the planar anchoring in the x direction. In equilibrium (minimum of the distortion energy), their radii are given by (10)

$$r_N^2 \approx 2R_m p \left( N - \frac{1}{2} - \frac{h_{min}}{p} \right) \qquad [1]$$

where $h_{min}$ is the minimal thickness of the gap, $R_m$ is the radius of curvature of the cylindrical mica sheets and N=1,2,3,... is the index of dislocation loops. This equation is valid when the tension of dislocations can be neglected (10) i.e. when the radius $r_N$ of cargo loops is much larger than the thickness $h$ of the gap between the mica sheets.

**Geometry of the necklace state, minimal loops.** Observations of the minimal loops in three samples with different cholesteric pitches (depending on the concentration of the chiral component CB15) are summarized in Figures 2c-e. They show that the diameter $D_{ml} = 2r_{ml}$ of the minimal loops is of the order of the cholesteric pitch $p$ which is smaller than the thickness $h$. In this case, the interaction with the mica surfaces is negligible so that such small dislocation loops of radius $r_{ml}$

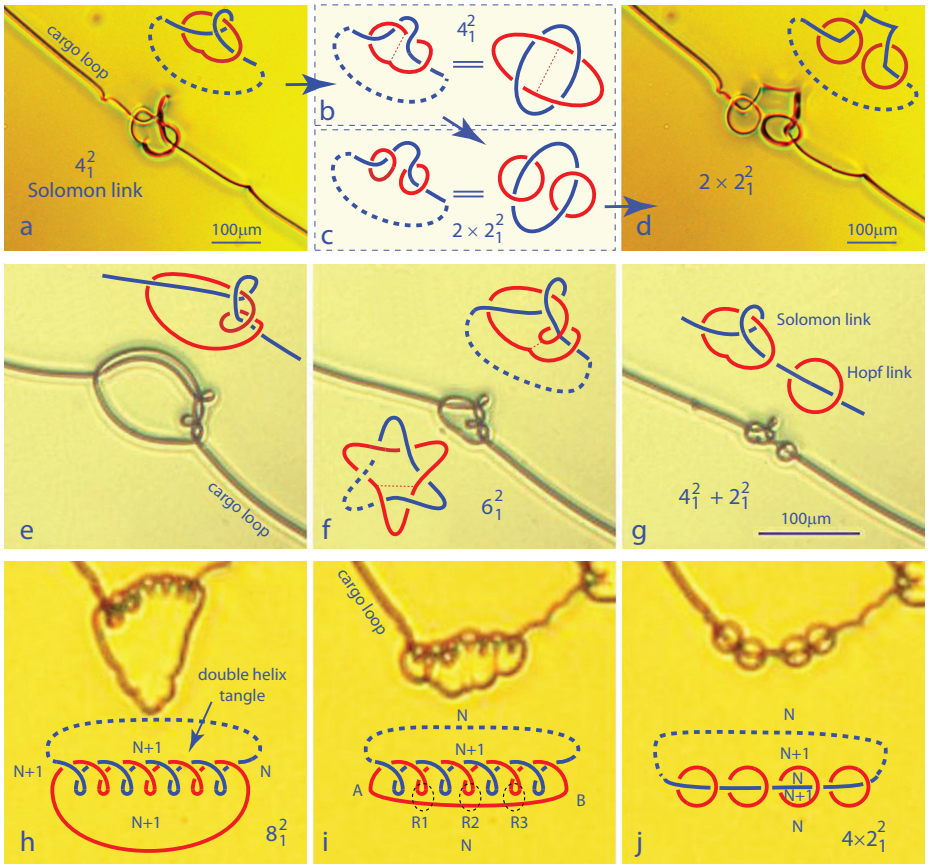


**Fig. 4.** Conservation of the linking number during the topological decay. a) The Solomon link $4_1^2$ inside the necklace state in a sample with a very large cholesteric pitch $p \approx 90\mu m$. a-d) Transformation of the Solomon link $4_1^2$ into two Hopf links $2_1^2$ driven by a shear deformation. f-g) Splitting of the $6_1^2$ link into one Solomon $4_1^2$ and one Hopf $2_1^2$ links. h-i) Splitting of the $8_1^2$ link into four Hopf $2_1^2$ links.

should collapse if they were submitted only to the action of the centripetal Laplace force

$$F_{Laplace} = -T/r_{ml} \qquad [2]$$

due to their tension $T$. This is the case of very small loops standing alone.

*The minimal loops tethered on kinks of cargo loops (see Figures 2 and 3) do not collapse because, as discussed in the SI Appendix Section "Diameter of minimal loops", they are submitted also to a repulsive interaction with kinks.*

**Stability of the necklace state.** Like knots and links made of dislocation loops, the necklace state is not stable but only metastable. The minimal loops tethered on the $+p$ kinks are threatened by lethal encounters with the $-p/2$ kinks as it is explained in the SI Appendix Section "Absorption of minimal loop due to a lethal encounter with a +p/2 kink". In practice, such encounters are very scarce so that in spite of its metastability the necklace state is long-lived.

## How the minimal loops are formed ?

In the Appendix Section "Evolution of the number of minimal loops" we report that the number of the tethered minimal loops evolves during the decay of the entanglements. Details of their birth are hidden at the beginning of the decay when the density of dislocation is too high but it becomes possible to identify them at the ultimate stage of the decay illustrated by the Figure 4 which shows that very often several minimal loops are born simultaneously.

**Splitting of the Solomon link.** The schemes drawn with blue and red lines in Figures 4a and b show that this penultimate configuration of the necklace state, in the absence of other minimal loops, would be equivalent to the Solomon link $4_1^2$. *A shear deformation* applied to this Solomon configuration of the necklace state transforms it into two Hopf links $2_1^2$ well visible in Figure 4d. This transformation is due to the splitting (rewiring) of the red loop in Figure 4b into two red loops in Figure 4c. Let us stress that in the absence of the shear and of encounters with free kinks, the Solomon link can persist indefinitely.

**Splitting of the $6_1^2$ link.** Another peculiar configuration of the necklace state is shown in Figure 4e. Here, the scheme drawn with blue and red lines unveils the topology of the $6_1^2$ link (in the absence of other minimal loops). Contrary to the Solomon configuration, this $6_1^2$ configuration is unstable and occurs only in a transitory manner during the decay sequence. The series of three pictures in Figures 4e, f and g shows that it splits into the Solomon $4_1^2$ link and the Hopf $2_1^2$ link.

**Splitting of the $8_1^2$ link.** The third example of an n-tuple birth is shown in Figures 4h-j. Here, the scheme drawn with blue and red lines unveils the topology of the $8_1^2$ link (in the absence of other minimal loops). From geometrical point of view this link can be seen as a helical tangle of two dislocations (17): the blue one is a part of a large cargo loop while the red one is a part of a much smaller loop tethered on the cargo loop in complex manner.

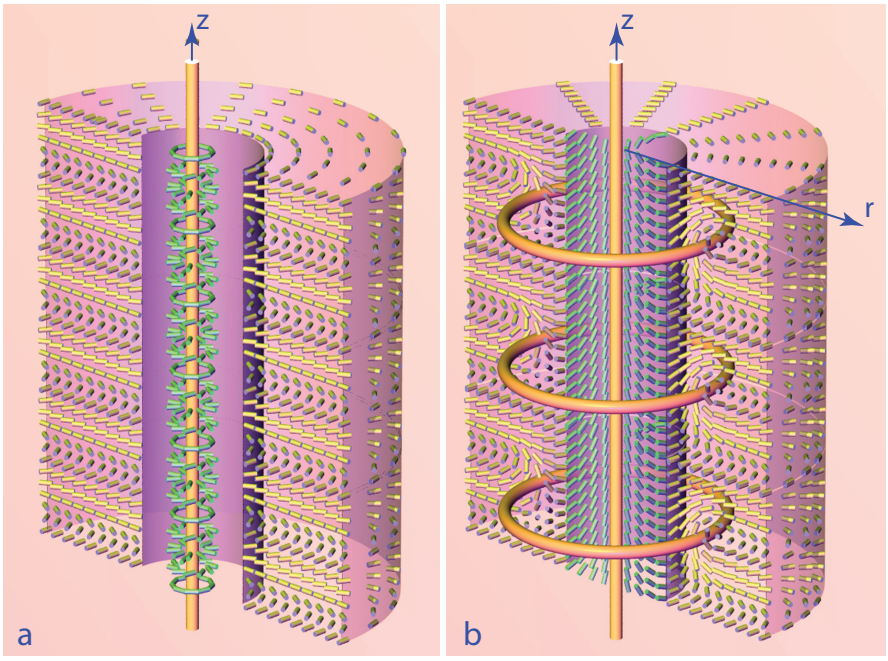


**Fig. 5.** The screw dislocation with the Burgers vector $\mathbf{b} = p\mathbf{e}_z$ parallel to cholesteric helix axis z. a) Singular version in which the director field $\mathbf{n} = [\cos\varphi, \sin\varphi, 0]$ is parallel to the (x,y) plane (22). b) Non-singular version in which the singularity is removed thanks to the "escape into the third dimension" (23). Remarkably, it has the topology of the necklace-like links reported in this paper.

**Conservation of the linking number during splitting of the $[2T]$ links into T [2] links.** In terms of the Conway notation (20, 21), in all above examples, the two components links $[2T]$ with T=1,2,3,... made of 2-tangles with 2T horizontal twists with numerator closure are rewired into necklaces made of T minimal loops tethered on cargo loops.

As far as we know, this type of rewiring is new; it does not involve as usual the crossings between the two components of the $[2T]$ link but only one of the two components and results in its splitting into smaller loops that remain linked with the second component. In the example of Figure 4i, three rewirings R1, R2 and R2 indicated with dotted circles split the red component of the two-component link $[8] = [2T]$ with the linking number T=4 into a five-components link made of T=4 red loops linked each once with the blue component. Let us emphasize that the rewiring $[2T] \to T[2]$ conserves the linking number T.

## Discussion and conclusions

**Necklace-like links made of dislocations.** From purely topological point of view, the necklaces made of dislocations are equivalent to a special class of multicomponent links made of several loops tethered on just one loop that we called cargo.

In our experiments, these links have very asymmetric shapes: the cargo loop is much larger than the tethered loops which have all a very small diameter of the order of the cholesteric pitch.

The large radius $r_N$ of the cargo loop is fixed by minimization of the elastic interactions with the surfaces of the mica sheets providing the planar anchoring. In a first approximation, this radius is such that the local thickness $h(r) = h_{min} + r_N^2/(2R_m)$ of the cylinder/cylinder gap is equal to $h_N = (N + 1/2)p$ (10). The radius $r_N$ decreases when $h_{min}$ grows, and tends to zero when $h_{min} = h_N$. For $h_{min} > h_N$ the cargo loops becomes unstable and collapses. The collapse of the cargo loop leads to the collapse of the necklace as a whole (see Figure S10 of the SI Appendix).

The radius $r_{ml} \approx p/2$ of the minimal loops tethered on the cargo loop is fixed by the balance between the Laplace centripetal force $T/r_{ml}$ due to the tension T of the tethered loop and the centrifuge repulsion force due to the elastic interaction between the tethered loop and the kink of the cargo loop. Obviously, the tethered loops loose their stability when the cargo loop collapses.

In conclusion, the necklace-like links made of the *non-singular dislocations* $b = p$ are remnants of the decay of arbitrarily complex entanglements of dislocations in cholesterics. The incomplete decay is due to the helical structure of cholesterics characterized by the helix pitch $p$ which determines the elastic interactions of dislocations with surfaces of the cylinder/cylinder gap as well as the elastic interactions between the non singular $b = p$ dislocations.

**Necklaces, links and knots made of disclinations in nematics.** The characteristic length $p$ is missing in interactions of the nematic disclinations with surfaces and between themselves. For this reason, entanglements of disclinations in nematics confined in the cylinder/cylinder gap always decay to the the defect-less state.

Let us note however that in the presence of cylindrical fibers or spherical inclusions immersed in nematics, the decay is incomplete because it leads, respectively, to disclination loops (unknots) tethered on fibers (24) and to knots or links tethered on inclusions (25). These topologically non trivial systems of defects owe their survival to the boundary conditions for orientation of molecules on surfaces of the cylindrical or spherical inclusions (anchoring of the director field).

**Necklace-like structure of screw dislocations in cholesterics.** The texture of the director field in the vicinity of the minimal loop tethered on the kink of the cargo loop from Figure 3 can be extended periodically in z direction as shown in Figure 5b.

It can be seen now as a non-singular variant of the singular model of the screw dislocation with the Burgers vector $\mathbf{b} = p\mathbf{e}_z$ parallel to cholesteric helix axis z represented in Figure 5a. This singular model was proposed for the first time by Bouligand and Kleman (see the scheme labeled "n=2, S=1 and m=0" in Figure 12 of the ref. (22)). The director field ($\mathbf{n} = [\cos\varphi, \sin\varphi, 0]$ parallel to the (x,y) plane) was generated by the Volterra process and has a linear singularity on the z axis corresponding to the singular disclination of rank m=1 (5)).

In Figure 5b, this singularity is removed thanks to the "escape into the third dimension" introduced by Williams et al. (23). Remarkably, the non-singular texture obtained by this means has the topology of the necklace-like links reported in this paper.

**Tethering of dislocation loops in smectics.** The necklace-like link of an edge dislocation loop pierced by a screw dislocation in smectics was considered by Kamien and Mosna in ref.(26). In this configuration, the edge dislocation loop acquires a helical shape so that it must be closed with a kink. Let us stress that in cholesterics, thanks to their helical symmetry, the edge dislocation loop tethered on a screw dislocation becomes flat.

In contradistinction with cholesterics, the edge and screw dislocations in smectics must have singular cores, like the superfluid vortices, because the order parameters of the smectic A and superfluid phases are the same: $\Psi = |\Psi| exp(i\varphi)$. We conjecture that for this reason the necklace-like links is smectics should be unstable.

**ACKNOWLEDGMENTS.** We thank Yves Pomeau and Bernard Derrida for the invitation to participate to the memorial issue of Comptes Rendus de l'Académie des Sciences (France) in honor of Gérard Toulouse. Writing our contribution stimulated greatly the recent experiments on the "objects with the double topological character" i.e. on the links and necklaces made of dislocation loops in cholesterics. We address our thanks for the hospitality to Yvan Smalyukh at the "International Institute for Sustainability with Knotted Chiral Metamatter (WPI-SKCM2)". The experimental setup tailored for production of the cholesteric dislocations in the cylinder/ cylinder mica wedges was inspired by discussions with M. Zeghal and built by V. Klein, J. Sanchez and S. Saranga. We also benefitted from discussions with Y. Pomeau, P.Oswald, Y. Smalyukh, O. Lavrentovich, A. Leforestier and C. Goldmann as well from the help of I. Settouraman, Y. Simon,M. Bottineau, J. Vieira and I. Nimaga.

1. G Toulouse, M Kleman, Principles of a classification of defects in ordered media. *J. de Physique Lettres* **37**, L–149 (1976).
2. M Kleman, O Lavrentovich, *Soft matter physics: an introduction.* (Springer, New york), 1 edition, (2001).
3. RP Feynman, Chapter ii application of quantum mechanics to liquid helium in *Progress in low temperature physics.* (Elsevier) Vol. 1, pp. 17–53 (1955).
4. D Kleckner, LH Kauffman, WT Irvine, How superfluid vortex knots untie. *Nat. Phys.* **12**, 650–655 (2016).
5. FC Frank, I. liquid crystals. on the theory of liquid crystals. *Discuss. Faraday Soc.* **25**, 19–28 (1958).
6. PG De Gennes, J Prost, *The physics of liquid crystals.* (Oxford university press) No. 83, (1993).
7. P Oswald, P Pieranski, *Nematic and cholesteric liquid crystals: concepts and physical properties illustrated by experiments.* (CRC press), (2005).
8. M Kleman, J Friedel, Lignes de dislocations dans les cholestériques. *J. de Phys.* **30**, C4–43–C4–53 (1969).
9. I Smalyukh, Review: knots and other new topological effects in liquid crystals and colloids. *Rep. Prog. Phys.* **83**, 1–46 (2020).
10. P Pieranski, M Godinho, Unknots, knots, links and necklaces made of dislocations in cholesterics. *Liq. Cryst.* pp. 1–32 (2024).
11. X Liu, RL Ricca, XF Li, Minimal unlinking pathways as geodesics in knot polynomial space. *Commun. Phys.* **3**, 136 (2020).
12. I Chuang, R Durrer, N Turok, B Yurke, Cosmology in the laboratory: Defect dynamics in liquid crystals. *Science* **251**, 1336–1342 (1991).
13. I Chuang, B Yurke, AN Pargellis, N Turok, Coarsening dynamics in uniaxial nematic liquid crystals. *Phys. Rev. E* **47**, 3343 (1993).
14. GP Bewley, KR Sreenivasan, The decay of a quantized vortex ring and the influence of tracer particles. *J. Low Temp. Phys.* **156**, 84–94 (2009).
15. F Grandjean, Sur l'existence des plans différenciés équidistants normaux l'axe optique dans les liquides anistropes. *Comptes Rendus Ac. Sc.* **268**, 71–74 (1921).
16. P Pieranski, Cholesteric dislocations in mica wedges. *Liq. Cryst. Rev.* **10**, 6–33 (2022).
17. P Pieranski, et al., Topological metadefects: tangles of dislocations. *Phys. Rev. Lett.* **131**, 128101 (2023).
18. P Pieranski, MH Godinho, Collisions of monopoles, disclinations and dislocations. *The Eur. Phys. J. Special Top.* pp. 1–21 (2024).
19. I Smalyukh, O Lavrentovich, Three-dimensional director structures of defects in grandjean-cano wedges of cholesteric liquid crystals studied by fluorescence confocal polarizing microscopy. *Phys. Rev. E* **6**, 051703 (2002).
20. JH Conway, An enumeration of knots and links, and some of their algebraic properties in *Computational problems in abstract algebra.* (Elsevier), pp. 329–358 (1970).
21. LH Kauffman, S Lambropoulou, On the classification of rational tangles. *Adv. Appl. Math.* **33**, 199–237 (2004).
22. Y Bouligand, M Kléman, Paires de disinclinaisons hélicoïdales dans les cholestériques. *J. de Physique* **31**, 1041–1054 (1970).
23. C Williams, P Pieranski, P Cladis, Nonsingular s=+ 1 screw disclination lines in nematics. *Phys. Rev. Lett.* **29**, 90 (1972).
24. M Dazza, L Cabeca, S Copar, MH Godinho, P Pieranski, Action of fields on captive disclination loops. *EPJE* **40**, 28 (2017).
25. U Tkalec, M Ravnik, S Čopar, S Žumer, I Muševič, Reconfigurable knots and links in chiral nematic colloids. *Science* **333**, 62–65 (2011).
26. RD Kamien, RA Mosna, The topology of dislocations in smectic liquid crystals. *New J. Phys.* **18**, 053012 (2016).